Nanoscale

ROYAL SOCIETY OF CHEMISTRY

MINIREVIEW

View Article Online
View Journal | View Issue

Cite this: *Nanoscale*, 2023, **15**, 13532

Ultrasound meets the cell membrane: for enhanced endocytosis and drug delivery

Zihao Wen,† Chen Liu,† Zihao Teng, Quanyi Jin, Zhihuan Liao, Xuan Zhu* and Shuaidong Huo *

Received 31st May 2023,
Accepted 14th July 2023

DOI: 10.1039/d3nr02562d

rsc.li/nanoscale

Endocytosis plays a crucial role in drug delivery for precision therapy. As a non-invasive and spatiotemporal-controllable stimulus, ultrasound (US) has been utilized for improving drug delivery efficiency due to its ability to enhance cell membrane permeability. When US meets the cell membrane, the well-known cavitation effect generated by US can cause various biophysical effects, facilitating the delivery of various cargoes, especially nanocarriers. The comprehension of recent progress in the biophysical mechanism governing the interaction between ultrasound and cell membranes holds significant implications for the broader scientific community, particularly in drug delivery and nanomedicine. This review will summarize the latest research results on the biological effects and mechanisms of US-enhanced cellular endocytosis. Moreover, the latest achievements in US-related biomedical applications will be discussed. Finally, challenges and opportunities of US-enhanced endocytosis for biomedical applications will be provided.

1. Introduction

Endocytosis is a fundamental cellular process that permits the internalization of extracellular molecules and particles, playing an integral role in numerous physiological functions, including nutrient uptake, signal transduction, and immune defense.[1,2] Endocytosis has been widely studied in the field of pharmaceutics to achieve better therapeutic effects with enhanced endocytic intracellular drug delivery.[3] Due to the selective expression of certain endocytic receptors involved in specific cells, drugs and target molecules attached to these receptors can increase drug uptake in targeted tissues or cells and reduce off-target effects.[4] Meanwhile, endocytosis can shield drugs from degradation by extracellular enzymes and enhance their stability during blood circulation, which can also be utilized to improve drug bioavailability by facilitating the transport of drugs across biological barriers.[5,6] In the clinic, aiming at ameliorating the pharmacokinetics of the drugs, reducing the frequency of dosing and improving patient compliance, modulation of endocytosis can be achieved by affecting extracellular signaling and receptor expression.[7] Therefore, optimizing the conditions of endocytosis has been of great interest for its positive impacts on the efficacy of the drug.[8,9] However, conventional drug delivery strategies lack valid modulation of the endocytic pathway and tend to be accompanied by inefficient cellular internalization.[10]

Emerging exogenous stimuli such as light, magnetic or electric fields, and ultrasound (US) are extensively studied to improve endocytosis efficiency and treatment benefits. Light offers precise spatial and temporal control. Although it can penetrate human tissues with minimal damage, capacitating their *in vivo* applications, the penetration depth is limited by light scattering and tissue absorption.[11] Magnetic fields are known for their non-invasive, remotely controlled focus on specific areas and for enabling high spatial resolution cell sorting and imaging. The disadvantages of magnetic fields are their drastic decrease in effectiveness with distance and the biocompatibility concern regarding magnetic materials.[12] Electric fields interrupt the cell membrane integrity or result in electroporation by bombarding charged particles that can promote cellular uptake and transport. Still, the distribution and penetration of electric fields in complex tissue structures are often limited.[13] Compared to the stimulation tools mentioned above, US is an excellent source of exogenous stimulation for cargoes' intracellular delivery due to its biosafety, deep tissue penetration, non-invasiveness, and precise spatiotemporal control.[14–16] This technique harnesses high-frequency sound waves to induce expansion-collapse of microbubbles (MBs) in solution, known as cavitation.[17,18] US-generated mechanical effects, such as microstreaming and shear forces, alter the physical properties of cells and extracellular

Fujian Provincial Key Laboratory of Innovative Drug Target Research, School of Pharmaceutical Sciences, Xiamen University, Xiamen 361102, China.
E-mail: zhuxuan@xmu.edu.cn, huosd@xmu.edu.cn
†These authors contributed equally to this work.

matrixes, create transient pores in cell membranes, and promote drug uptake; such a phenomenon is called sonoporation.[19–21] On the one hand, sonoporation forms membrane pores that result in a direct inward drug flow and affects the ion pumps on the membrane surface to reduce its outward drug excretion.[22] On the other hand, the artificial addition of microbubbles can lower the threshold of US-induced cavitation, thus enhancing the efficiency and positively influencing the endocytic behavior of cells.[23] Cell membranes are the cellular structures that are most vulnerable to and interact with US. The mechanical pressure exerted by the US significantly affects the morphology and fluidity of the cell membrane *via* interruption of lipid and protein movement and organization. At the same time, the membrane potential is altered upon exposure of ion channels and cytoskeletons to mechanical forces. These membrane changes effectively enhance the internalization of extracellular substances by cells and play a key role in applications such as drug delivery.[24,25]

In this review, we summarized the biophysical changes of US-exerted impacts on cell membranes and mechanisms during sonoporation-mediated cellular endocytosis (Fig. 1). Moreover, recent progress in studying sonoporation-provoked bioeffects for delivering active ingredients to overcome severe diseases is highlighted. Finally, the challenges and opportunities of US-enhanced drug delivery for biomedical applications and the remaining gaps in related mechanistic research are discussed.

2. Mechanisms involved in US-enhanced endocytosis

The US-induced sonoporation effect contributes to increased cellular endocytosis of foreign substances. In this section, we discuss the current mechanisms of US-induced physicochemical changes in cell membranes, such as the formation and repair of cell membrane pores, the variation of ion channels of the membrane, *etc.* (Table 1).

2.1. US-induced membrane perforation

Cell membranes are vulnerable to injuries under extreme physical and chemical environments induced by cavitation, including physical disruption of the morphology, chemical erosion of components, high-temperature melting of membranes, and oxidative stress.[25] The heat generated by US is claimed to increase drug endocytosis by modulating membrane permeability, especially in multidrug-resistant cancer cells.[26,27] Among them, the most significant damage is from forming membrane pores. Thus, investigating the exact sizes of membrane pores is a starting point for understanding the mechanism. Previous research using scanning electron microscopy (SEM) has allowed the observation of irregular membrane pores ranging from a hundred nanometres to a few micrometers in diameter.[28,29] Khayamian *et al.* applied SEM and confocal imaging to observe membrane pore formation in

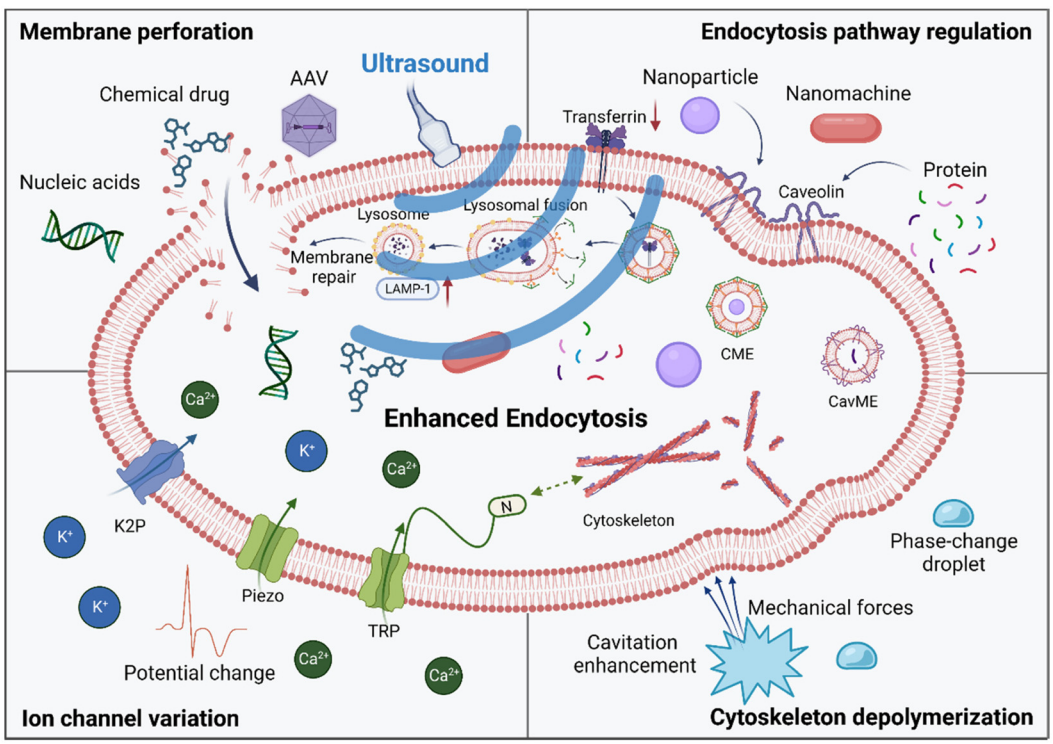

Fig. 1 Schematic illustration of biological effects and mechanism behind US meets the cell membrane, including US-induced membrane perforation, endocytosis pathway regulation, ion channel variation, and cytoskeleton depolymerization, for enhanced endocytosis and drug delivery. Created with BioRender.com.

Table 1 Ultrasound with different parameters induced cell membrane variation of multiple cell types

Cell type	Ultrasound parameters (frequency, intensity, exposure duration)	Characteristics	Ref.
Rat mammary carcinoma cells; human embryonic kidney cells; bovine endothelial monolayer cells	Frequency (20 Hz–16 MHz)	Ultrasound-induced membrane pores range from a hundred nanometres to a few micrometers in diameter	28, 29
HUVEC cells; MCF-7 cells	Frequency (20 kHz), intensity (0.9 and 1.8 W cm^{-2})	Different cell mechanical flexibility shows diverse sonoporation	30
MCF-7 cells	Frequency (1 MHz); intensity (0.9 and 1.8 W cm^{-2}); exposure duration (5–60 s)	Membrane pore size was related US exposure times and sound pressures	31, 32
Rat cardio myoblast (H9c2) cells; HeLa cells	Frequency (1 MHz; 1.5 MHz)	Ca^{2+} is a factor in membrane repair	33, 34
Xenopus oocytes	Frequency (1.06 and 0.96 MHz)	The rate of repair correlates with Ca^{2+} concentration	35, 36
Breast cancer cells (SK-BR-3)	Frequency (40 kHz); exposure duration (10–30 s)	MB-produced significantly greater cell membrane porosity	47
Mammary breast cancer cells (MDA-MB-231)	Frequency (1 MHz); exposure duration (2–20 s)	Microbubbles' oscillations under ultrasound activation could modulate ionic transports	51
HeLa cells; K562 cells	Frequency (1 MHz); exposure duration (20 s–60 s)	Permanent depolarization triggers programmed cell death	52, 54
Endothelial cells	Frequency (1 MHz), intensity (3 or 2.1 W cm^{-2})	Ultrasound-induced Ca^{2+} transiently passed through TRPV4 channels	58
Neuron cells	Frequency (300 or 670 kHz)	The US affects calcium-selective mechanosensitive ion channels (TRPC1, TRPP2, and TRPM4)	59
Mouse primary cortical neurons; mammalian cells	Frequency (1, 2, or 7 MHz)	US-sensitive channel hsTRPA1	60
Nerve cells	Frequency (0.5 or 2 MHz)	Ultrasound-influenced Piezo-1 channels for calcium influx	62, 63
Human melanoma cells (BLM cells)	Frequency (1 MHz); exposure duration (30 s)	Membrane deformation of microbubbles may trigger endocytosis by mechanical stimulation of the cytoskeleton	75
ZR-75-30 human breast carcinoma cells	Frequency (1 MHz)	Disruption of actin cytoskeleton organization	76
B16 melanoma cells	Frequency (1.5 MHz); exposure duration (20 min)	A Rab5-Rac1 pathway involved ultrasound-mediated endocytosis and cell motility	77
MCF-7 cells, CT4 cells	Frequency (100 kHz–1 MHz)	A kinetic model of the cancer cytoskeleton at low frequencies	79

two cell lines (HUVEC and MCF-7) at different US intensities (0.9 and 1.8 W cm^{-2}) (Fig. 2A).[30] Factors affecting the membrane pore size are complex and varied, of which US parameters are considered crucial, and longer US exposure times and higher sound pressures will worsen membrane destruction.[31] For instance, Qiu *et al.* showed that the pores on the membrane became severely irrecoverable with increasing duration and intensity of the US, ranging from 150 nm to 1 μm.[32] They also proposed a significant positive correlation between membrane pore sizes and inertial cavitation doses (ICDs).

US-mediated pore formation promotes the free flow of various ions through cell membranes, particularly extracellular Ca^{2+}. Several researchers have investigated the roles of ions in membrane resealing after US treatment, and the concentration of Ca^{2+} is found to be a vital membrane repair factor.[33,34] Zhou *et al.* found that the rate of membrane recovery decreased with Ca^{2+} concentration and completely ceased in the absence of Ca^{2+}. The minimum concentration threshold for successful membrane repair was reported to be 0.54 mM.[35] Conversely, in the presence of extracellular Ca^{2+}, the cell membrane reseals more rapidly.[36] For other organelles, Ca^{2+} affects calcium-dependent proteins and the cytoskeletons and stimulates the self-fusion of plasma membranes or lysosomes, all essential for cell membrane repair.[37] Moreover, Ca^{2+} will also affect cholesterol-rich cell membrane compartments and trigger their spontaneous vesicles, leading to the formation of endocytic vesicles, which will in turn enhance the efficiency of cellular uptake.[38]

The extent of membrane damage by US is then considered relevant to the success of membrane repair. The self-repair of membranes is a crucial aspect of US-enhanced endocytosis, and it maintains the homeostatic balance of the cell while avoiding the entry of harmful substances and unwanted ions into the cell. Membrane repair mainly consists of endocytosis-induced membrane repair[39] and exocytosis-linked vesicular patching,[40] Endocytosis is responsible for removing damaged cell membranes, while exocytosis rebuilds new cell membranes, restoring the intact morphology and mechanical properties of the plasma membrane.[41] Endocytosis is considered to repair membrane pores in minor damage, but extensive membrane damage requires exocytosis and lysosomal plaques for reconstruction.[42] Some researchers found that only holes smaller than 0.2 μm can be successfully resealed.[43] Still, a study by Hu *et al.* revealed that membrane perforations <30 μm^2 repaired themselves within 1 minute after US treatment, whereas membrane perforations >100 μm^2 remained damaged for half an hour. In addition, the time of resealing the membranes determined the viability of the cells after US. Another publication indicated that only cells with pores that

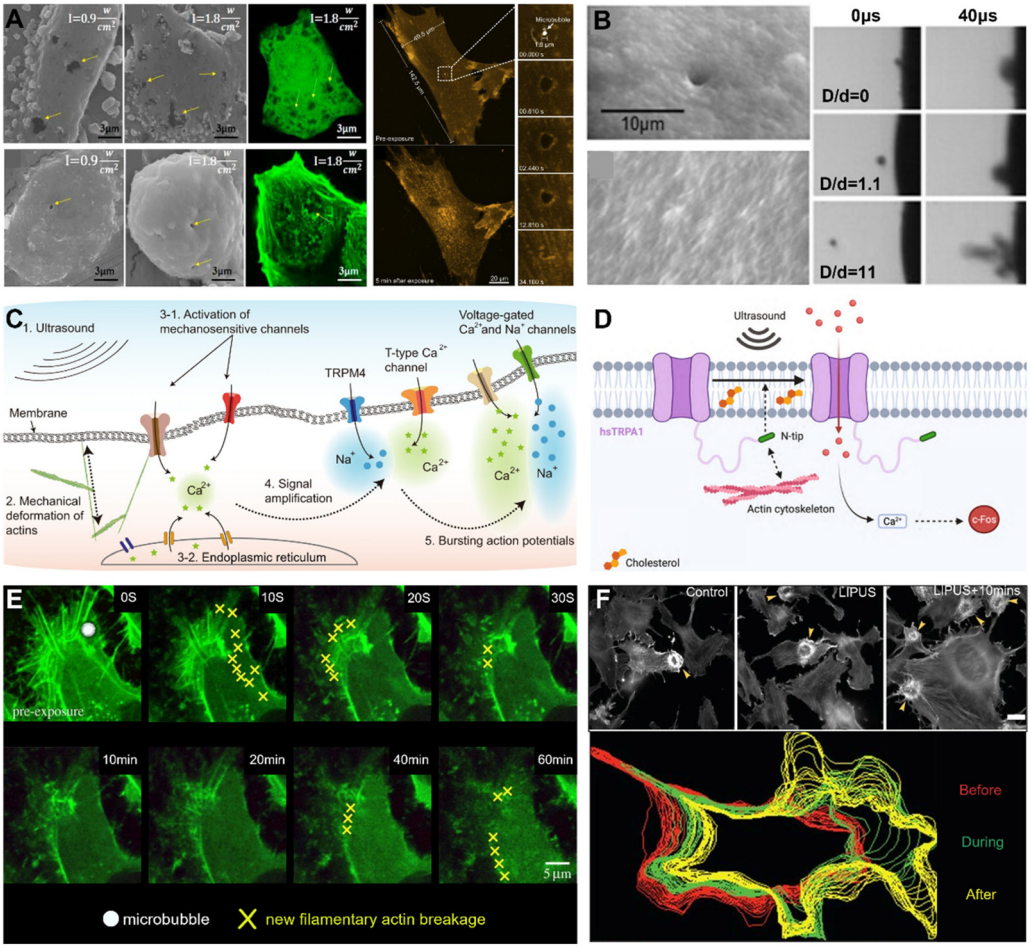

Fig. 2 Representative studies of the US-mediated cell membrane variation: phenomena and mechanism. A. SEM images and confocal microscopy imaging after US stimulation of cells, showing damage (yellow arrow in left) and repair (right) of cell membranes. Reproduced from ref. 30 with permission from Elsevier 2018 and ref. 44 with permission from Elsevier 2013. B. US-induced pore and cavitation at different microbubble-membrane distances (D/d). The effective range of cavitation on the membrane porosity D/d = 0.75. Reproduced from ref. 49 with permission from Elsevier 2012. C. Molecular pathway illustration of US-activated mechanosensitive ion channels (TRPP1/2, TRPC1 and Piezo1). Reproduced from ref. 59 with permission from Springer Nature 2022. D. Mechanism of actions of hsTRPA1 exposed to US in which the N-terminal tip, actin cytoskeleton and cholesterol increase intracellular calcium and c-Fos expression. Reproduced from ref. 60 with permission from Springer Nature 2022. E. Time-series induction of actin cytoskeletal network disruption by sonoporation observed by fluorescent labelling, the white circle at 0 s indicates the location where cavitation occurs and the yellow cross marker means filamentary actin loss compared to the previous time point. Reproduced from ref. 76 with permission from Royal Soc 2014. F. Live imaging of US-induced formation of actin-based circular dorsal ruffles (CDRs), and automated detection of changes in the cell membrane morphology with cytoskeletal rearrangement recorded by QuimP. Reproduced from ref. 77 with permission from The Company of Biologists 2017.

resealed within one minute remained viable after US treatment (Fig. 2A).[44] Nevertheless, it is noteworthy that non-resealing pores do not necessarily affect cell viability,[45] and scientists need more in-depth research to explain this conflict.

Although studies have shown that prolonged high-intensity US can lead to irrecoverable damage, employing MBs is a promising strategy that lowers the US threshold of triggering cavitation and increases temporary porosity.[46] Hence, the MBs are another critical factor in sonoporation. On the one hand, some researchers used fluorocarbons (C_3F_8 or SF_6) to fill MB-produced cell membrane porosity that would be significantly greater than air-filled cell membrane porosity, suggesting that droplets prone to a phase change could be more advantageous.[47] On the other hand, the researchers found that large bubbles increased the pore radius from 24.6 nm to 34.5 nm compared to smaller ones under the same US pulse.[48] Besides, there is a need to consider both the diameter of the MBs (d) and the distance between the MBs and the cell membranes (D), designating the ratio between the two (d/D) as the reference indicator for the severity of the membrane damage instead of either value alone (Fig. 2B).[49]

2.2. US-induced variation of membrane potentials and ion channels

Membrane potentials are crucial in many fundamental physiological processes, such as cell cycle regulation, cell volume

maintenance, proliferation, muscle contraction, and wound healing.[50] Notably, US treatment can also significantly influence membrane potentials.

Varying durations of membrane hyperpolarization induced by US have been observed in different cells. In the MDA-MB-231 cell line, Tran *et al.* demonstrated that hyperpolarization of cell membranes persists until US exposure ceases due to the stimulation of surrounding MBs and the activation of calcium-gated BKCa stretch channels.[51] However, permanent depolarization was observed in HeLa cells,[52] possibly related to differences in membrane ion channels between cell lines. In a separate study, Vasan *et al.* developed a biomechanical model in HEK cells that accurately predicts the membrane voltage during US exposure, which aligns with previously reported data.[53] Moreover, researchers have observed that permanent cell membrane depolarization can trigger programmed cell death.[54,55]

The on-and-off status of membrane ion channels determines the differences aforementioned in membrane potentials. The ion channels that are most vulnerable to US intervention are known as mechanosensitive channels (MSCs), a large family with many members: Piezo channels, transient receptor potential (TRP) ion channels, large mechanosensitive channels (MscL), and small mechanosensitive channels (MscS), *etc*.[56,57] For TRP channels, several studies have recently attempted to explain their mechanism of actions under US stimulation, such as that by Liao *et al.* showed that Ca^{2+} transiently passed through receptor potential vanilloid 4 (TRPV4) channels in response to US stimulation and activated the PKC-δ pathway, leading to the dissociation of connexins (ZO-1 and occlusion) and ultimately improving BBB permeability.[58] And Shapiro's group investigated the effects of US on neurons by exciting primary murine cortical neurons, revealing that specific calcium-selective mechanosensitive ion channels (TRPC1, TRPP2, and TRPM4) mediated the exciting process rather than cavitation, which updated the understanding of the effects of US on ion channels (Fig. 2C).[59] Similar studies found that human transient receptor potential A1 (hsTRPA1), a manipulable US-sensitive channel in mammalian cells, required its N-terminal tip region to interact with cholesterol for US-induced ion gating (Fig. 2D).[60] Another family that has been extensively studied in neuronal and brain diseases is the Piezol family. In the mouse primary cortex, Qiu *et al.* investigated the role of Piezo1 with the intervention of US. They showed that heterologous and endogenous Piezo1 was activated, initiating calcium influx and the expression of essential proteins such as phosphorylated-CaMKII, phosphorylated-CREB and c-Fos.[61] Utilizing Piezo1-targeting MBs could enable Ca^{2+} ions in-flow and sensitize N2A cells and primary cultured neurons to respond in low US intensity, providing a safer strategy for US neuromodulation.[62] In a recent study, Zhu and colleagues have demonstrated at the level of *in vivo* regulation and animal behavior that Piezo1 is a crucial mediator in modifying neuronal behavior with US.[63]

Also, US was found to modulate potassium and sodium mechanosensitive ion channels (channels of the two-pore-domain potassium family (K2P) including TREK-1, TREK-2, TRAAK; Na_V 1.5), with an average current ratio of up to 23%.[64] These mechanosensitive ion channels are also suggested to have a different mechanism under US exposure, with a low probability of opening without membrane tension. However, when the membrane stretches with mechanical force intervention, the shape changes of the structural proteins within the channel are energetically favorable, tending to a channel opening state.[65]

2.3. US-mediated endocytosis pathway regulation

Cell membrane proteins play a crucial role in cellular endocytosis. Several endocytosis pathways are involved for materials/cargoes to enter cells,[66] and US has been reported to mainly affect caveolae-dependent endocytosis and clathrin-coated pit-mediated endocytosis (CME; clathrin and dynamin-dependent). Current research has identified different pathways related to proteins/acceptors that US could affect, leading to endocytic behavior changes of cells.

In the formation and stabilization of caveolae, caveolin-1 is a key structural component. Deng *et al.* found that the expression of caveolin-1 was upregulated through US combined with a dose of microbubble treatment in a rat model, which could facilitate endocytosis.[67] Similar findings were also demonstrated in human umbilical vein endothelial cells. Pulsed diagnostic US was able to selectively activate endothelial caveolar-mediated internalization of recombinant glutathione-*S*-transferase (GST)-Tat11-EGFP fusion protein. This effect was achieved by the phosphorylation of caveolin-1 without disrupting the integrity of the plasma membrane. Using different molecule weights of dextran, researchers also indicated that the upregulation of caveolin-1 significantly enhances the endocytosis of larger cargoes (500 kDa), while showing no significant effect on smaller molecule cargoes (3 kDa, 70 kDa).[68] In addition, colocalization of 500 kDa dextran with clathrin was discovered through fluorescence imaging, which supported the role of clathrin-coated pit-mediated endocytosis after US exposure to the cardio myoblast cells.[69] In another study, Tardoski *et al.* first found that the mechanical stress induced by low-intensity US resulted in a statistically significant increase of clathrin and enhanced bisphosphonate uptake into MCF-7 cells after US treatment.[27] Research also revealed that US treatment significantly improved CME, and a 37.28 ± 4.0% decrease in cell membrane transferrin receptors (TfRs) was observed.[70] Meanwhile, a 53.0 ± 16.1 fold increase of the lysosomal associated membrane protein 1 (LAMP-1) was also measured in the intact cytoplasmic membrane, indicating that US caused an increase in lysosomal fusion with the plasma membrane, which may be related to the membrane repair mechanism involving lysosomes and exocytosis mentioned above.

Furthermore, US can down-regulate the expression of receptors on the cell membrane, such as reducing the amount of CD19 on lymphocytes or decreasing the expression of P-glycoprotein.[71,72] The former is mainly due to mechanical

damage caused by the cavitation effect of US, while the latter is mainly attributed to the impact of US on the integrity of intracellular genes, thus affecting the expression of relevant proteins, increasing endocytosis or reducing drug resistance. In short, US irradiation could dynamically induce cell membrane surface protein changes, which is closely related to US parameters and the membrane recovery process. However, the exact molecular biological mechanisms are not yet evident, and further in-depth research is still needed in the future.

2.4. US-induced cytoskeleton depolymerization

Cytoskeleton fibers play a vital role in many essential intracellular biological activities, such as endocytosis or exocytosis. As a key component in maintaining cellular morphology/structure, cytoskeleton fibers are composed of microtubules, microfilaments, and intermediate filaments (IFs).[73] During the endocytosis process, microfilaments pull the vesicles containing the engulfed particles into the cell for transporting substances.[74] Under US irradiation, shear and radiation forces are applied to the cell membrane and inevitably impact cytoskeletons, leading to "cell fractures" and cytoskeleton depolymerization.[17]

Numerous studies have reported cytoskeleton alteration after US treatment. De Cock *et al.* observed cell membrane deformation/breakage through real-time confocal microscopy under US irradiation, which may be caused by reorganization/disruption of the cytoskeleton.[75] More precisely, Chen *et al.* demonstrated the rapid breakdown of the F-actin network near the perforation site by ultrasonically triggered rupture of a single targeted MBs in the cell membrane (Fig. 2E).[76] Furthermore, with the structural tensor analysis method combined with exponential decay regression, the characteristic time for actin network breakdown was estimated to be around a few seconds, and the velocity changes were directly related to the cell entry rate of the sonic repair tracer. In another study, the mechanosensitive focal adhesion (FA) protein vinculin can sense US *via* cell–matrix adhesion, which could rearrange the actin and regulate the Rab5-Rac1 pathway to control US-mediated endocytosis and cell motility (Fig. 2F).[77] In addition, Jia *et al.* developed a spatiotemporal dynamic model of the actin cytoskeletons based on the HUVEC cell line, and they proposed that the kinetic process of acoustic pressure-induced actin cytoskeleton fracture includes three stages: expansion, contraction resealing, and recovery.[78] Meanwhile, in cells with reversible sonoporation, the dynamics of the disrupted actin cytoskeletons would be partially synchronized with the dynamics of the perforated plasma membrane, depending on the size of the perforation. Similar studies developed a kinetic model of the cancer cytoskeleton at low frequencies: cellular dynamics, statistical mechanics of network elasticity, and "life-and-death" dynamics were applied to describe the damage and repair processes of the cytoskeletons, and the simplified model was applied to theoretically predict the ablation effect of low-frequency US on cancer cells.[79]

3. US-enhanced cellular endocytosis strategies for biomedical applications

US-induced sonoporation causes a complex series of physiological changes in the cell membranes contributing to enhanced endocytosis. These reversible changes can facilitate the efficient delivery of various chemicals, biological molecules, or nanocarriers. In this section, we sort and highlight the widespread use of US in promoting the intracellular delivery of multiple types of cargoes (Table 2).

3.1. Chemical drugs and nucleic acid sequence

US-mediated drug delivery and gene transfection have been well-established and widely used to treat various diseases. The assistance of US can enhance the endocytosis of small molecule drugs to nerve cells. Endocytosis of small molecule drugs to nerve cells can be enhanced by US assistance. In the Parkinson's disease (PD) model, the intervention of US increased the drug concentration of gastrodin and provided optimal neuroprotection.[80] Similarly, in the Alzheimer's disease (AD) model, US significantly enhanced the therapeutic effect of the small molecule methylene blue, reducing amyloid-β (Aβ) plaque deposition and neuronal damage within the hippocampus.[81] The combination of anti-cancer drugs such as temozolomide[82] and pirarubicin[83] with US has also been shown to enhance their cellular endocytosis and improve the effectiveness of chemotherapy.

In other small molecule drug therapy models, US can increase the drug concentration of poly hexamethylene biguanide by up to 2.63 times and thus treat parasitic keratitis,[84] as well as using US to promote the uptake of trehalose by red blood cells, increasing the recovery of viable cells after lyophilization and rehydration, thus enabling long-term storage of blood.[85] Besides, Aryal *et al.* found that the molecular weight of chemical drugs may not be a crucial factor for endocytosis. They observed a significant increase in the uptake of both small (~1 kDa) and large (~155 kDa) dextran from the cerebrospinal fluid to the perivascular space after US treatment of rat brains (Fig. 3A).[86] Similarly, another study revealed that small (~0.6 kDa) and large molecules (~150 kDa) share similar levels of delivery efficiency under refined parameters.[87]

As hydrophilic substances with high molecular weight, nucleic acid sequences have difficulty crossing the cell membranes. Compared to other transfection methods, US exhibits excellent transfection ability, which can significantly increase the intracellular delivery of nucleic acids. For example, a high level of transgene expression in combined plasmid hepatocytes was reported. An optimized pulse sequence US condition was applied with immunomodulation to treat hemophilia A with mild transient liver injury.[88] Similar strategies have been well discussed in several recent reviews.[89–91]

3.2. Carrier-based drug delivery

With the development of nanotechnology and its beneficial role in drug delivery, various nanocarriers have been widely

Table 2 Ultrasound with different parameters enhanced cellular endocytosis for biomedical applications

Delivery type	Drug or drug carrier	Ultrasound parameters (frequency, intensity, exposure time)	Application	Ref.
Molecular	Gastrodin	Frequency (1 MHz); exposure time (60 s)	FUS enhanced GAS delivery for optimal neuroprotective effects	80
	Methylene blue (MB)	Frequency (1.1 MHz); exposure time (120 s)	FUS/MB combination treatment reduced the number of Aβ plaques	81
	Temozolomide (TMZ)	Frequency (200 kHz); exposure time (210 s)	FUS-mediated disruption of BBB for an increase of TMZ	82
	Pirarubicin	Frequency (5 MHz)	Ultrasound-triggered microbubble cavitation enhanced pirarubicin concentration for intravesical chemotherapy	83
	Poly hexamethylene biguanide	Frequency (400 kHz or 600 kHz); intensity (0.5 or 0.8 W cm^{-2}); exposure times (1–5 min)	Ultrasound enhanced corneal permeability to polyhexamethylene biguanide	84
	Trehalose	Frequency (2.5 MHz)	Ultrasound-mediated trehalose loading for superior recovery of viable erythrocytes	85
	Dextran	FUS, frequency (650 kHz)	Ultrasound enhanced small and large molecular agents into the perivascular space	86, 87
Carrier-based drug delivery	Adeno-associated viruses (AAVs)	Frequency (0.58 MHz); exposure times (180 s)	FUS-assisted AAVs delivery for degenerative diseases	91, 92
	Inorganic-based nanoparticles (Dox@L@FeHD)	FUS	FUS-induced constant temperature triggering the *in situ* stepwise Dox release	94
	Liposomes	FUS	Ultrasound transiently opens the blood–brain barrier and delivers liposomes	95, 96
	Micelles	Frequency (1 MHz); intensity (1.5 W cm^{-2})	Ultrasound-induced production of Fe^{2+} from Fc, $^{\bullet}OH$, and $^{1}O_2$ for sonodynamic and chemodynamic therapy	98
	Micro/nanorobots	Frequency (2.66 MHz, 330–550 kHz)	Ultrasound-propelled micro/nanorobots for biomedical applications	99, 100
	US-responsive bacteria (URB)	Frequency (960 Hz)	Ultrasound-controlled expression of exogenous genes by URB	101
Microbubble-assisted drug delivery	αvβ3-targeted MBs with a C_4F_{10} gas core	Frequency (2 MHz)	Internalized microbubbles facilitate ultrasound-induced drug delivery through pores and tunnels	103
	MBs-assisted edaravone	Frequency (1 Hz)	FUS/MB-enhanced delivery technology for amyotrophic lateral sclerosis (ALS)	104
	MBs-nanoliposomal particle	Frequency (5–12 MHz)	Microbubble-nanoliposomal particle effectively facilitates the delivery of Cas9/sgRNA protein by US activation for restoring hair growth	105
	Gemcitabine (GEM) and perfluoropentane (PFP) loaded liposomes	Frequency (3 MHz); intensity (2 W cm^{-2})	Ultrasonic-cavitation-based liposomes have superior tumor accumulation and deep penetration, generating effective antitumor activity	108
	Dex/PFP@LIPs-BMS-α	Frequency (1 MHz), intensity (0.8, 1.6, 2.4 W cm^{-2})	LIFU responsive nano-delivery system specific delivers dexamethasone (Dex) to podocyte targets and reduces systemic side effects	109
	Proteins-loaded PFC nanoemulsions	Frequency (1 MHz), intensity (0.1–2.0 W cm^{-2})	Ultrasound-sensitive fluoro-protein nanoemulsions for on-demand cytosolic delivery of proteins	110
	Genetically encoded gas vesicles (GVs)-expressing bacteria	Frequency (300, 334, 670 kHz, 3 MHz)	GV-expressing bacteria combined with genetic engineering technology and US to control the occurrence of cavitation and achieve accurate drug delivery	111, 112

used in disease diagnosis and treatments. US-induced sonoporation has further propelled the development of various nanocarriers for drug delivery. These sono-sensitive systems could enhance the delivery of active therapeutic ingredients into specific cells, such as adeno-associated viruses (AAVs), inorganic-based nanoparticles, liposomes, micelles and micro/nanorobots.

With targeted stimulation by focused ultrasound (FUS), recombinant AAVs are widely deployed as gene transfection vectors for neurological disorders. Kofoed *et al.* systematically compared the gene delivery effects of different AAVs combined with FUS. They discovered that the properties of the AAV serotype, the parameters of FUS and the intrinsic properties of the target brain tissue all affect the gene delivery efficiency. This study provides a reliable choice for designing safe and effective gene delivery strategies.[92] Furthermore, Touahri *et al.* have extended this approach to Müller glial cells to stimulate their repair potential in degenerative diseases.[93]

In addition, the extensive application of US-responsive materials spurred the development of inorganic-based nanomaterials, which were designed in various shapes and sizes for

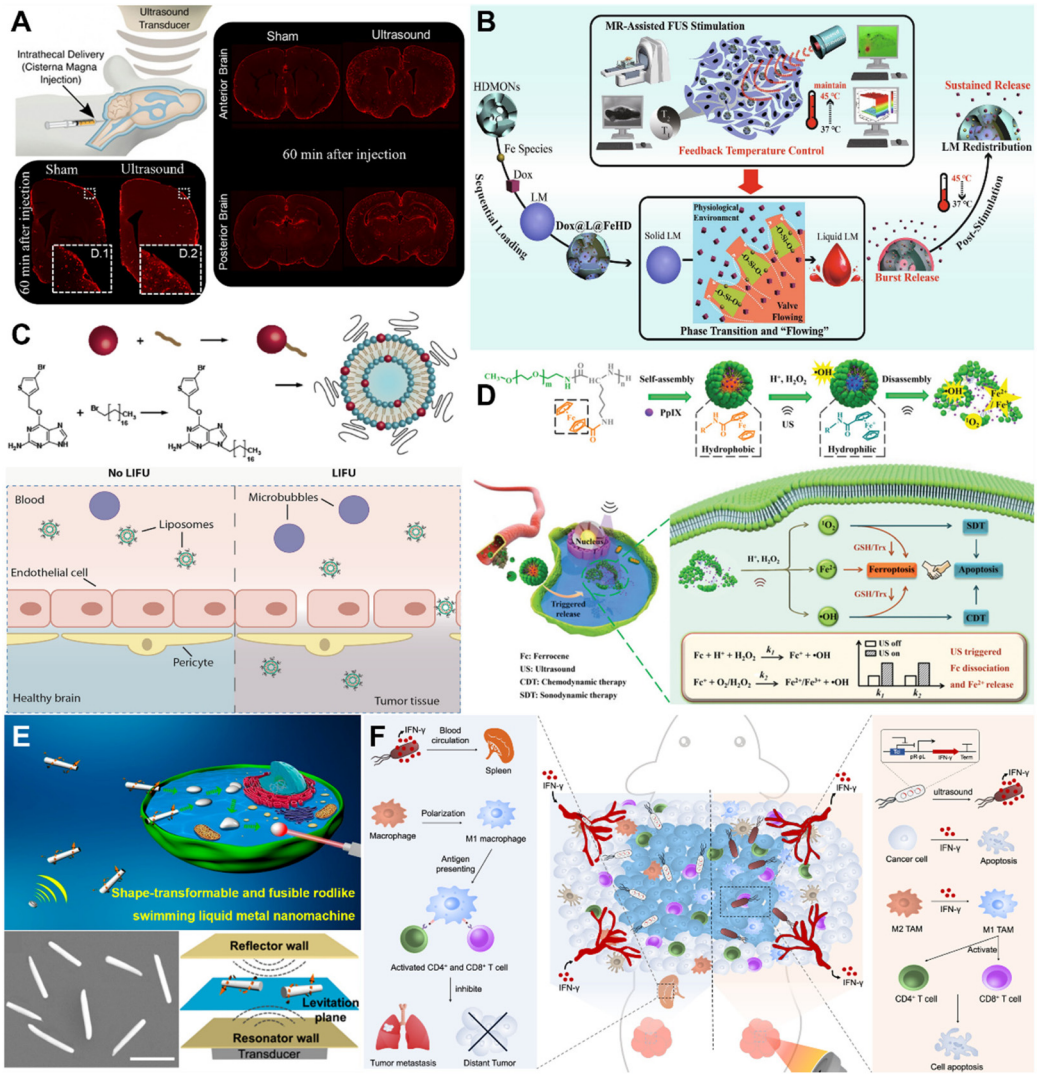

Fig. 3 Representative examples of small molecule drug-, gene-, and carrier-based delivery assisted by US. A. Non-invasive transcranial US increased the uptake of both small (~1 kDa) and large (~155 kDa) molecules. Reproduced from ref. 86 with permission from Elsevier 2022. B. Schematic diagram of the synthesis of Dox@L@FeHD nanoparticles based on mesoporous silica and its progressive release under/after FUS stimulation. Reproduced from ref. 94 with permission from Elsevier 2021. C. LIFU-mediated disruption of the BBB for selectively delivering a liposomal LP-O^6BTG-C18 derivative to the target region. Reproduced from ref. 95 with permission from Elsevier 2019. D. Schematic illustration of the mechano-responsive leapfrog micelles (PpIX@MFc) for releasing active ingredients on demand during US irradiation for site-specific cancer treatment. Reproduced from ref. 98 with permission from WILEY-VCH 2022. E. Liquid metal gallium nanomachines (LGNMs) propelled by US and actively pierce into HeLa cells. Reproduced from ref. 100 with permission from American Chemical Society 2018. F. Design of the US-responsive bacterium (URB) loaded with the cytokine interferon-gamma (IFN-γ) for enhanced antitumor effects. Reproduced from ref. 101 with permission from Springer Nature 2022.

drug delivery. A recent publication revealed that hollow dendritic mesoporous organosilica nanoparticles (HDMONs) were utilized to load doxorubicin (Dox) and L-menthol (LM) to obtain a US-responsive nanoplatform Dox@L@FeHD. With an *in vivo* FUS stimulation, Dox@L@FeHD exhibited a sustained temperature of 45 °C in the target tumor region, consequently initiating a gradual release of Dox and promoting the uptake of drugs by tumor cells (Fig. 3B).[94]

As a classic US-responsive material, liposomes could load a variety of chemical/biological drugs to improve the blood circulation time and biocompatibility. Papachristodoulou *et al.* confirmed that a liposomal O^6-(4-bromothenyl)guanine (O^6BTG) derivative could be efficiently delivered under low-intensity pulsed FUS, and then target the methyltransferase (MGMT) and sensitize murine cells to temozolomide for prolonged survival of glioblastoma patients (Fig. 3C).[95] Another liposome coated with cleavable polyethylene glycol (PEG) and loaded with Dox, showed excellent tumor accumulation, extravasation, and therapeutic efficiency in exposure to US.[96] In one cryotropic hydrogel system, US has also been shown to disrupt electrostatic interactions in the gel system, promoting host dendritic cells (DCs) binding to the immunogen.[97]

Furthermore, micellar systems, as another group of commonly used drug delivery vehicles, demonstrated their crucial role in US-responsive drug delivery. For example, a mechano-responsive polymeric micellar system could achieve the release of active ingredients on demand and enhanced delivery to cancer cells during US irradiation. The physically encapsulated sonosensitizer (PpIX) and covalently linked ferrocene could produce hydroxyl radicals ($^{\bullet}OH$) and singlet oxygen ($^{1}O_2$) to cause the accumulation of lipid peroxidation (LPO) for site-specific cancer treatment (Fig. 3D).[98]

Apart from the abovementioned studies, other novel US-assist vehicles have been reported. US-driven micro and nanoscale robots perform better cellular internalization than common passive nanosystems. A research group presented US-propelled gold nanowire (Au NW) nanomotors with red blood cell membrane-cloaked perfluorocarbon nanoemulsions (RBO-PFC), which could penetrate the cell membranes and deliver oxygen to cells.[99] Meanwhile, Wang *et al.* reported a liquid metal gallium nanomachine (LGNM), which could be propelled by US and actively pierce HeLa cells. Such an acoustically propelled rodlike machine showed great potential for theranostics (Fig. 3E).[100] US-responsive bacteria (URB) have also been reported as a novel gene carrier that can load the cytokine interferon-gamma (IFN-γ), while can be acoustically remote controlled by designing temperature-driven genetic switches that enhance the anti-tumor effects of the URB *in vitro* and *in vivo* (Fig. 3F).[101]

3.3. Microbubble-assisted drug delivery

Microbubbles (MBs), as compressible entities, can undergo contraction, expansion, and rupture when subjected to ultrasonic compression, resulting in superior cavitation efficiency and acoustic radiation. Therefore, utilizing MB-assisted nanosystems to perturb cell membranes is a promising approach to overcoming biological barriers and enhancing drug delivery. To this end, gas-containing MBs, phase-change droplets transformed into MBs, and genetically encoded gas vesicles are usually used.

Gas-containing microbubbles refer to small, spherical structures that consist of a gas core encapsulated by a thin shell. Klazina Kooiman group developed an ultra-high-speed imaging system for the detailed information of US-responsive MBs. The 20 Mfps interleaving timing could provide the knowledge of MBs interacting with cells under US.[102] Recently, this group also applied the αvβ3-targeted MBs with a C_4F_{10} gas core to reveal that the MBs influenced the 3D morphology of the endothelial cell membrane and the effects of MB internalization on the oscillation threshold for cavitation and drug delivery outcomes. The oscillation of the MBs can create both pores and tunnels, with the former facilitating intracellular drug delivery, and the latter enhancing both intracellular and transcellular permeation (Fig. 4A).[103] Related studies discovered that FUS combined with MB could enhance the brain delivery of edaravone and further improve the neuromuscular functions along with rescued muscle atrophy (Fig. 4B).[104] Meanwhile, Ryu *et al.* designed an MB-nanoliposomal particle as a carrier for delivering the Cas9/sgRNA nucleoprotein complex. When activated by the US, it efficiently facilitates local delivery of the complex to dermal cells in hair follicles of animals with androgenetic alopecia. Cas9/sgRNA delivered by MB-nanoliposomal efficiently recognizes and specifically edits target genes both *in vitro* and *in vivo*, thereby restoring hair growth (Fig. 4C).[105] Additionally, US-mediated MB destruction (UMMD) was applied for ischemia–reperfusion injury, wound healing and vascular bioeffects.[106,107]

Furthermore, the acoustic droplet vaporization (ADV) effect could enhance the mechanical force during the collapse of cavitation MBs. Typical acoustic droplets including 2,2′-azobis[2-(2-imidazolin-2-yl)propane]dihydrochloride (AIPH), a gas generating polymer (poly(BL-pro)), perfluoropentane and so on. In other words, the phase-change droplets produced ultrasonic cavitation effect can break down biological barriers and achieve effective drug delivery. For example, Wang *et al.* explored gemcitabine (GEM) and perfluoropentane (PFP) loaded liposomes which could transform nanodroplets into MBs *via* phase transition under US irradiation. Then the surface corona could be decorticated and expose the targeting peptide to achieve enhanced tumor accumulation and penetration, resulting in effective anti-tumor activities in patient-derived tumor xenografts in a variety of tumor models (Fig. 4D).[108] In another example, multifunctional nanoparticles called Dex/PFP@LIPs-BMS-α were fabricated, which demonstrated the FUS-induced gas-phase transformation of PFP.[109] Noteworthily, Sloand *et al.* reported a novel method for loading proteins into the fluorine interior of PFC nanoemulsions to achieve spatiotemporal control in US-mediated cell transduction. This approach utilized a series of fluorinated hydrophilic chemical tags (FTags) with fluorinated masking capabilities, allowing them to bind instantaneously to proteins and disperse efficiently in the fluorine medium. This approach maintained the folded and biologically active state of the proteins (Fig. 4E).[110]

In addition, due to the challenge that exogenous/synthetic MBs/phase-change droplets have limited efficiency for targeting extravascular biomolecules, Shapiro's groups showed that genetically encoded gas vesicles (GVs, gas-filled protein nanostructures) could intelligently regulate cellular endocytosis and biomedical application. They first introduced this GV acoustic reporter gene into mammalian cells to generate US contrast signals. Therefore, US visualization and high-resolution imaging of cells at less than 0.5% bulk density were achieved.[111] After that, they developed GV-expressing bacteria that could reach the deep regions of the tumor and act as key intracellular nuclei for cavitation, resulting in mechano-therapeutic effects that inhibit tumor growth under FUS treatment (Fig. 4F).[112] The timing and location of cavitation can be controlled specifically with the aid of US by constructing cells that can express GVs through genetic engineering technology. The combination of genetic engineering technology and US can more effectively control the occurrence of cavitation and achieve accurate drug delivery. Most recently, through the expression of GVs within mammalian cells, they have achieved precise physical manipulation of specific cells by US. The GVs

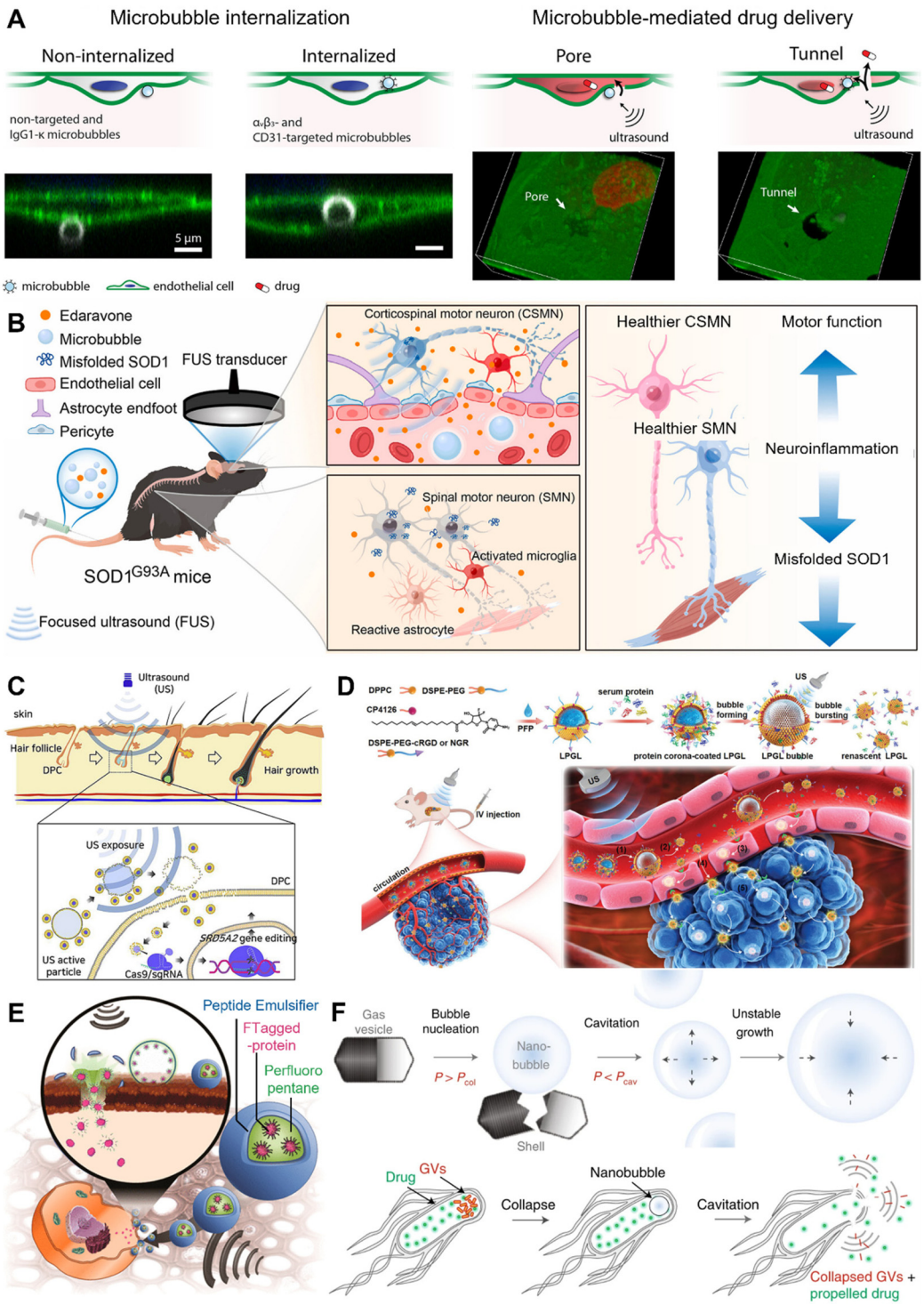

Fig. 4 Representative examples of MB-assisted nanosystems for enhanced cellular endocytosis and drug delivery. A. Schematic diagram of MB internalization and the MB induced pore and tunnel for endocytosis and drug delivery. Reproduced from ref. 103 with permission from Elsevier 2022. B. Schematic illustration of FUS combined with the MB enhanced delivery of edaravone. Reproduced from ref. 104 with permission from Elsevier 2023. C. Schematic diagram of MB-nanoliposome particles delivering Cas9/sgRNA into dermal cells *via* US induced sonoporation. Reproduced from ref. 105 with permission from Elsevier 2020. D. Schematic illustration of PFP-loaded LPGL nanoparticles could transform into MBs *via* phase-change process for enhanced tumor delivery under irradiation. Reproduced from ref. 108 with permission from WILEY-VCH 2023. E. Schematic illustration of PFC-loaded nanoemulsions delivering proteins in a spatiotemporally precise and quantitative manner through the cavitation of acoustic vaporized microbubbles. Reproduced from ref. 110 with permission from American Chemical Society 2020. F. Schematic illustration of intracellular GV-seeded cavitation and cell disruption. Reproduced from ref. 112 with permission from Springer Nature 2021.

could reverse the acoustic contrast of the cell and amplify the acoustic radiation force (ARF) on the cell, allowing them to move in response to variations in pressure, and provide a new strategy for selective acoustic manipulation.[113]

4. Conclusion and outlook

This review summarizes recent mechanistic research and groundbreaking applications of US-induced biophysical and biochemical effects on cell membranes. Studies on enhanced endocytosis *via* US-triggered permeabilization were classified and discussed, mainly involving the uptake of small-molecule or biomolecule drugs, nanocarriers, and microbubble-assisted nanosystems. Undoubtedly, the US provides a powerful strategy for enhancing cell endocytosis for drug delivery.

Although the recent progress of US-based strategies has provided great promise in enhancing drug delivery, we must acknowledge several challenges in accelerating the translation of US to clinical applications. One of the most critical issues is the biosafety. Even though the US treatment has superior biocompatibility, cell membrane pores induced by US treatment are too large to be restored when they are more significant than 100 μm^2, which will affect the regular physiological activity of cells or even viability.[44] For this reason, appropriate acoustic parameters urgently need to be investigated and determined for generating reversible membrane pores. In addition to biosafety, improving the effectiveness of US-induced cavitation is also a challenge. The most common strategy is to introduce gas-loaded nanoparticles or phase-change droplets to provide more microbubbles and strengthen the cavitation effect. With the clinical application of various gas-loaded nanoparticles and droplets, such as Opsion, Definity, Sonazoid, and Lumason, there will be more development of gas- or droplet-based systems for US-enhanced drug delivery.[114,115] In addition, using targeting microbubbles or controlling the distance between the microbubble and the cell membrane can achieve better results.

So far, multiple strategies have been studied to improve the safety and effectiveness of US.[116,117] However, there are few reports on the precise regulation of US *in vivo* to reach the target position rather than studies at the cellular level. To achieve this goal, the first problem is to quantify the US-induced *in vivo* bioeffect precisely, such as the sonoporation degree. Even the intensity of fluorescent molecules internalized by cells can be quantified using imaging tools,[30] but assessing the variation of biological signals *in vivo* is challenging. Furthermore, controlling the number of microbubbles around the cells is highly desirable to obtain a definite bioeffect. Recently, genes that encode gas vesicles could be transfected into the cells of interest to achieve a certain number of microbubbles, which has excellent potential in US-assisted precision medicine.[112,113] Besides, the US penetration ability is mainly related to its frequency, tissue attenuation coefficient, and patient heterogeneity. And the tissue penetration depth usually limits the enhancement of ultrasound-induced endocytosis. Choosing ultrasound with lower frequency, high penetration, and focused ultrasound that can concentrate energy to one point will help improve ultrasound penetration depth and achieve sonoporation with lower acoustic intensity and higher spatial selectivity *in vivo*, which is a reliable strategy for future clinical applications.

In addition to US-assisted enhancement of endocytosis, US-induced mechanical forces can also be an excellent method to modulate the cell membrane's physicochemical transformation, thus selectively interfering with the chemical bonds of some proteins or ion channels, thus quantitatively achieving the expected biological effects.[16,118] However, even though the concept is relatively mature, practical research is still limited by current ultrasonic instruments that cannot be precisely modulated, and its application *in vitro* or *vivo* still faces complex problems, which is another important research direction that requires effort to make breakthroughs.

Although the clinical transformation of US-enhanced endocytosis faces many challenges, we believe that, with the continuous optimization of US-related strategies, these problems will be overcome. Shortly, we anticipate that more attempts to develop US-based methods will be encouraging for enhancing drug delivery, which will provide valuable references for improving the drug efficacy for precision medicine.

Abbreviations

US	Ultrasound
SEM	Scanning electron microscopy
ICD	Inertial cavitation doses
MBs	Microbubbles
BKCa	Calcium-activated potassium channel
MSCs	Mechanosensitive channels
TRP	Transient receptor potential
MscL	Large mechanosensitive channels
MscS	Small mechanosensitive channels
TRPV4	Transient receptor potential vanilloid 4
CME	Clathrin-coated pit-mediated endocytosis
CavME	Caveolae mediated endocytosis
GST	Glutathione-*S*-transferase
TfR	Transferrin receptor
LAMP-1	Lysosomal associated membrane protein 1
IF	Intermediate filament
FA	Focal adhesion
HUVECs	Human umbilical vein endothelial cells
CDRs	Circular dorsal ruffles
PD	Parkinson's disease
AD	Alzheimer's disease
Aβ	Amyloid-β
AAV	Adeno-associated virus
FUS	Focused ultrasound
URB	Ultrasound-responsive bacterium
BBB	Blood–brain barrier
Dox	Doxorubicin
LM	L-Menthol

HDMONs	Hollow dendritic mesoporous organosilica nanoparticles
O^6BTG	Liposomal O^6-(4-bromothenyl)guanine
MGMT	Methyltransferase
FEG	Polyethylene glycol
DCs	Dendritic cells
PpIX	Protoporphyrin IX
LPO	Lipid peroxidation
Au NW	Gold nanowire
RBO-PFC	Red blood cell membrane-cloaked perfluorocarbon nanoemulsions
LGNMs	Liquid metal gallium nanomachines
URB	US-responsive bacteria
IFN-γ	Interferon-gamma
UMMD	Ultrasound-mediated microbubble destruction
ADV	Acoustic droplet vaporization
AIPH	2,2′-Azobis[2-(2-imidazolin-2-yl)propane] dihydrochloride
GEM	Gemcitabine
PFP	Perfluoropentane
LPGLs	Transcytosis-targeting-peptide-decorated reconfigurable liposomes
PFC	Perfluorocarbon
FTags	Fluorinated hydrophilic chemical tags
GVs	Gas vesicles
ARF	Acoustic radiation force
LIFU	Low-intensity pulsed focused ultrasound

Conflicts of interest

There are no conflicts to declare.

Acknowledgements

This work was supported by the National Natural Science Foundation of China (NSFC) (no. 82001959 and 82273872) and the Nanqiang Outstanding Young Talents Program from Xiamen University.

References

1 S. Sigismund, L. Lanzetti, G. Scita and P. P. Di Fiore, *Nat. Rev. Mol. Cell Biol.*, 2021, **22**, 625–643.
2 M. Kaksonen and A. Roux, *Nat. Rev. Mol. Cell Biol.*, 2018, **19**, 313–326.
3 B. Banushi, S. R. Joseph, B. Lum, J. J. Lee and F. Simpson, *Nat. Rev. Cancer*, 2023, **23**, 450–473.
4 D.-D. Wang and X.-N. Zhang, *J. Controlled Release*, 2021, **333**, 418–447.
5 J. J. Rennick, A. P. R. Johnston and R. G. Parton, *Nat. Nanotechnol.*, 2021, **16**, 266–276.
6 M. J. Mitchell, M. M. Billingsley, R. M. Haley, M. E. Wechsler, N. A. Peppas and R. Langer, *Nat. Rev. Drug Discovery*, 2021, **20**, 101–124.
7 Y. Sato, Y. Sakurai, K. Kajimoto, T. Nakamura, Y. Yamada, H. Akita and H. Harashima, *Macromol. Biosci.*, 2017, **17**, 1600179.
8 S. Patel, J. Kim, M. Herrera, A. Mukherjee, A. V. Kabanov and G. Sahay, *Adv. Drug Delivery Rev.*, 2019, **144**, 90–111.
9 N. Chen, Y. He, M. Zang, Y. Zhang, H. Lu, Q. Zhao, S. Wang and Y. Gao, *Biomaterials*, 2022, **286**, 121567.
10 O. S. Fenton, K. N. Olafson, P. S. Pillai, M. J. Mitchell and R. Langer, *Adv. Mater.*, 2018, **30**, 1705328.
11 W. Zhao, Y. Zhao, Q. Wang, T. Liu, J. Sun and R. Zhang, *Small*, 2019, **15**, 1903060.
12 S. Sengupta and V. K. Balla, *J. Adv. Res.*, 2018, **14**, 97–111.
13 N. Rahoui, B. Jiang, N. Taloub and Y. D. Huang, *J. Controlled Release*, 2017, **255**, 176–201.
14 L. Tu, Z. Liao, Z. Luo, Y.-L. Wu, A. Herrmann and S. Huo, *Exploration*, 2021, **1**, 20210023.
15 S. Huo, Y. Zhou, Z. Liao, P. Zhao, M. Zou, R. Göstl and A. Herrmann, *Chem. Commun.*, 2021, **57**, 7438–7440.
16 S. Huo, P. Zhao, Z. Shi, M. Zou, X. Yang, E. Warszawik, M. Loznik, R. Göstl and A. Herrmann, *Nat. Chem.*, 2021, **13**, 131–139.
17 I. Lentacker, I. De Cock, R. Deckers, S. De Smedt and C. Moonen, *Adv. Drug Delivery Rev.*, 2014, **72**, 49–64.
18 Y. Wang and D. S. Kohane, *Nat. Rev. Mater.*, 2017, **2**, 17020.
19 I. Beekers, M. Vegter, K. R. Lattwein, F. Mastik, R. Beurskens, A. F. van der Steen, N. de Jong, M. D. Verweij and K. Kooiman, *J. Controlled Release*, 2020, **322**, 426–438.
20 Y. Yang, Q. Li, X. Guo, J. Tu and D. Zhang, *Ultrason. Sonochem.*, 2020, **67**, 105096.
21 F. M. Kashkooli, A. Jakhmola, T. K. Hornsby, J. J. Tavakkoli and M. C. Kolios, *J. Controlled Release*, 2023, **355**, 552–578.
22 A. Bouakaz, A. Zeghimi and A. A. Doinikov, in *Therapeutic Ultrasound*, 2016, pp. 175–189.
23 K. Kooiman, S. Roovers, S. A. Langeveld, R. T. Kleven, H. Dewitte, M. A. O'Reilly, J.-M. Escoffre, A. Bouakaz, M. D. Verweij and K. Hynynen, *Ultrasound Med. Biol.*, 2020, **46**, 1296–1325.
24 B. Geers, H. Dewitte, S. C. De Smedt and I. Lentacker, *J. Controlled Release*, 2012, **164**, 248–255.
25 D. Przystupski and M. Ussowicz, *Int. J. Mol. Sci.*, 2022, **23**, 11222.
26 Y. Liu, C.-W. Cho, X. Yan, T. K. Henthorn, K. O. Lillehei, W. N. Cobb and K.-Y. Ng, *Pharm. Res.*, 2001, **18**, 1255–1261.
27 S. Tardoski, E. Gineyts, J. Ngo, A. Kocot, P. Clézardin and D. Melodelima, *Ultrasound Med. Biol.*, 2015, **41**, 2740–2754.
28 Z. Fan, R. E. Kumon and C. X. Deng, *Ther. Delivery*, 2014, **5**, 467–486.
29 N. Kudo, K. Okada and K. Yamamoto, *Biophys. J.*, 2009, **96**, 4866–4876.

30 M. A. Khayamian, M. Baniassadi and M. Abdolahad, *Ultrason. Sonochem.*, 2018, **41**, 619–625.
31 F. Yang, N. Gu, D. Chen, X. Xi, D. Zhang, Y. Li and J. Wu, *J. Controlled Release*, 2008, **131**, 205–210.
32 Y. Qiu, Y. Luo, Y. Zhang, W. Cui, D. Zhang, J. Wu, J. Zhang and J. Tu, *J. Controlled Release*, 2010, **145**, 40–48.
33 Z. Fan, R. E. Kumon, J. Park and C. X. Deng, *J. Controlled Release*, 2010, **142**, 31–39.
34 C. Jia, L. Xu, T. Han, P. Cai, C. Alfred and P. Qin, *Ultrasound Med. Biol.*, 2018, **44**, 1074–1085.
35 Y. Zhou, J. Shi, J. Cui and C. X. Deng, *J. Controlled Release*, 2008, **126**, 34–43.
36 C. X. Deng, F. Sieling, H. Pan and J. Cui, *Ultrasound Med. Biol.*, 2004, **30**, 519–526.
37 M. A. Hassan, P. Campbell and T. Kondo, *Drug Discovery Today*, 2010, **15**, 892–906.
38 C. Rentero, P. Blanco-Muñoz, E. Meneses-Salas, T. Grewal and C. Enrich, *Int. J. Mol. Sci.*, 2018, **19**, 1444.
39 V. Idone, C. Tam, J. W. Goss, D. Toomre, M. Pypaert and N. W. Andrews, *J. Cell Biol.*, 2008, **180**, 905–914.
40 A. Reddy, E. V. Caler and N. W. Andrews, *Cell*, 2001, **106**, 157–169.
41 P. Qin, T. Han, C. Alfred and L. Xu, *J. Controlled Release*, 2018, **272**, 169–181.
42 R. K. Schlicher, J. D. Hutcheson, H. Radhakrishna, R. P. Apkarian and M. R. Prausnitz, *Ultrasound Med. Biol.*, 2010, **36**, 677–692.
43 P. L. McNeil and R. A. Steinhardt, *Annu. Rev. Cell Dev. Biol.*, 2003, **19**, 697–731.
44 Y. Hu, J. M. Wan and C. Alfred, *Ultrasound Med. Biol.*, 2013, **39**, 2393–2405.
45 T. van Rooij, I. Skachkov, I. Beekers, K. R. Lattwein, J. D. Voorneveld, T. J. Kokhuis, D. Bera, Y. Luan, A. F. van der Steen and N. de Jong, *J. Controlled Release*, 2016, **238**, 197–211.
46 M. Wang, Y. Zhang, C. Cai, J. Tu, X. Guo and D. Zhang, *Sci. Rep.*, 2018, **8**, 3885.
47 Y.-Z. Zhao, Y.-K. Luo, C.-T. Lu, J.-F. Xu, J. Tang, M. Zhang, Y. Zhang and H.-D. Liang, *J. Drug Targeting*, 2008, **16**, 18–25.
48 Z. Fan, H. Liu, M. Mayer and C. X. Deng, *Proc. Natl. Acad. Sci. U. S. A.*, 2012, **109**, 16486–16491.
49 Y. Zhou, K. Yang, J. Cui, J. Ye and C. Deng, *J. Controlled Release*, 2012, **157**, 103–111.
50 L. Abdul Kadir, M. Stacey and R. Barrett-Jolley, *Front. Physiol.*, 2018, **9**, 1661.
51 T. Tran, S. Roger, J.-Y. Le Guennec, F. Tranquart and A. Bouakaz, *Ultrasound Med. Biol.*, 2007, **33**, 158–163.
52 P. Qin, L. Xu, Y. Hu, W. Zhong, P. Cai, L. Du, L. Jin and C. Alfred, *Ultrasound Med. Biol.*, 2014, **40**, 979–989.
53 A. Vasan, J. Orosco, U. Magaram, M. Duque, C. Weiss, Y. Tufail, S. H. Chalasani and J. Friend, *Adv. Sci.*, 2022, **9**, 2101950.
54 L. Zhao, Y. Feng, A. Shi, Y. Zong and M. Wan, *Ultrasound Med. Biol.*, 2015, **41**, 2755–2764.
55 J. Li, L. Ma, X. Liao, D. Liu, X. Lu, S. Chen, X. Ye and T. Ding, *Front. Microbiol.*, 2018, **9**, 2486.
56 J. M. Kefauver, A. B. Ward and A. Patapoutian, *Nature*, 2020, **587**, 567–576.
57 S. E. Murthy, A. E. Dubin and A. Patapoutian, *Nat. Rev. Mol. Cell Biol.*, 2017, **18**, 771–783.
58 W.-H. Liao, M.-Y. Hsiao, Y. Kung, H.-L. Liu, J.-C. Béra, C. Inserra and W.-S. Chen, *J. Adv. Res.*, 2020, **26**, 15–28.
59 S. Yoo, D. R. Mittelstein, R. C. Hurt, J. Lacroix and M. G. Shapiro, *Nat. Commun.*, 2022, **13**, 493.
60 M. Duque, C. A. Lee-Kubli, Y. Tufail, U. Magaram, J. Patel, A. Chakraborty, J. Mendoza Lopez, E. Edsinger, A. Vasan and R. Shiao, *Nat. Commun.*, 2022, **13**, 600.
61 Z. Qiu, J. Guo, S. Kala, J. Zhu, Q. Xian, W. Qiu, G. Li, T. Zhu, L. Meng and R. Zhang, *iScience*, 2019, **21**, 448–457.
62 X. Shen, Z. Song, E. Xu, J. Zhou and F. Yan, *Ultrason. Sonochem.*, 2021, **73**, 105494.
63 J. Zhu, Q. Xian, X. Hou, K. F. Wong, T. Zhu, Z. Chen, D. He, S. Kala, S. Murugappan, J. Jing, Y. Wu, X. Zhao, D. Li, J. Guo, Z. Qiu and L. Sun, *Proc. Natl. Acad. Sci. U. S. A.*, 2023, **120**, e2300291120.
64 J. Kubanek, J. Shi, J. Marsh, D. Chen, C. Deng and J. Cui, *Sci. Rep.*, 2016, **6**, 24170.
65 B. Sorum, R. A. Rietmeijer, K. Gopakumar, H. Adesnik and S. G. Brohawn, *Proc. Natl. Acad. Sci. U. S. A.*, 2021, **118**, e2006980118.
66 J. J. Rennick, A. P. Johnston and R. G. Parton, *Nat. Nanotechnol.*, 2021, **16**, 266–276.
67 J. Deng, Q. Huang, F. Wang, Y. Liu, Z. Wang, Z. Wang, Q. Zhang, B. Lei and Y. Cheng, *J. Mol. Neurosci.*, 2012, **46**, 677–687.
68 R. Pandit, W. K. Koh, R. K. Sullivan, T. Palliyaguru, R. G. Parton and J. Götz, *J. Controlled Release*, 2020, **327**, 667–675.
69 B. D. Meijering, L. J. Juffermans, A. van Wamel, R. H. Henning, I. S. Zuhorn, M. Emmer, A. M. Versteilen, W. J. Paulus, W. H. van Gilst and K. Kooiman, *Circ. Res.*, 2009, **104**, 679–687.
70 F. Fekri, R. C. Delos Santos, R. Karshafian and C. N. Antonescu, *PLoS One*, 2016, **11**, e0156754.
71 M. Aryal, K. Fischer, C. Gentile, S. Gitto, Y.-Z. Zhang and N. McDannold, *PLoS One*, 2017, **12**, e0166061.
72 A. A. Brayman, M. L. Coppage, S. Vaidya and M. W. Miller, *Ultrasound Med. Biol.*, 1999, **25**, 999–1008.
73 A. F. Pegoraro, P. Janmey and D. A. Weitz, *Cold Spring Harbor Perspect. Biol.*, 2017, **9**, a022038.
74 R. Duncan and S. C. Richardson, *Mol. Pharm.*, 2012, **9**, 2380–2402.
75 I. De Cock, E. Zagato, K. Braeckmans, Y. Luan, N. de Jong, S. C. De Smedt and I. Lentacker, *J. Controlled Release*, 2015, **197**, 20–28.
76 X. Chen, R. S. Leow, Y. Hu, J. M. Wan and A. C. Yu, *J. R. Soc., Interface*, 2014, **11**, 20140071.
77 P. Atherton, F. Lausecker, A. Harrison and C. Ballestrem, *J. Cell Sci.*, 2017, **130**, 2277–2291.

78 C. Jia, J. Shi, T. Han, C. Alfred and P. Qin, *Ultrasound Med. Biol.*, 2022, **48**, 760–777.
79 E. Schibber, D. Mittelstein, M. Gharib, M. Shapiro, P. Lee and M. Ortiz, *Proc. R. Soc. A*, 2020, **476**, 20190692.
80 Y. Wang, K. Luo, J. Li, Y. Liao, C. Liao, W.-S. Chen, M. Chen and L. Ao, *Front. Cell. Neurosci.*, 2022, **16**, 884788.
81 H. J. Choi, M. Han, B. Jung, Y.-R. Hong, S. Shin, S. Lim, E.-H. Lee, Y. K. Kim and J. Park, *Biomedicines*, 2022, **10**, 3191.
82 S. H. Park, M. J. Kim, H. H. Jung, W. S. Chang, H. S. Choi, I. Rachmilevitch, E. Zadicario and J. W. Chang, *Front. Oncol.*, 2020, **10**, 1663.
83 N. Sasaki, Y. Ikenaka, K. Aoshima, T. Aoyagi, N. Kudo, K. Nakamura and M. Takiguchi, *Front. Pharmacol.*, 2022, **13**, 837754.
84 B. Karpinecz, N. Edwards and V. Zderic, *J. Ultrasound Med.*, 2021, **40**, 2561–2570.
85 C. S. Centner, E. M. Murphy, M. C. Priddy, J. T. Moore, B. R. Janis, M. A. Menze, A. P. DeFilippis and J. A. Kopechek, *Biomicrofluidics*, 2020, **14**, 024114.
86 M. Aryal, M. M. Azadian, A. R. Hart, N. Macedo, Q. Zhou, E. L. Rosenthal and R. D. Airan, *J. Controlled Release*, 2022, **349**, 434–442.
87 C. S. Centner, J. T. Moore, M. E. Baxter, K. Yaddanapudi, P. J. Bates and J. A. Kopechek, *Ultrasound Med. Biol.*, 2023, **49**, 90–105.
88 S. Song, M. J. Lyle, M. L. Noble-Vranish, D. M. Min-Tran, J. Harrang, W. Xiao, E. C. Unger and C. H. Miao, *Mol. Ther. – Nucleic Acids*, 2022, **27**, 916–926.
89 N. Zhang, J. Wang, J. Foiret, Z. Dai and K. W. Ferrara, *Adv. Drug Delivery Rev.*, 2021, **178**, 113906.
90 A. P. Walsh, H. N. Gordon, K. Peter and X. Wang, *Adv. Drug Delivery Rev.*, 2021, **179**, 113998.
91 M. R. Schwartz, A. C. Debski and R. J. Price, *J. Controlled Release*, 2021, **339**, 531–546.
92 R. H. Kofoed, C. L. Dibia, K. Noseworthy, K. Xhima, N. Vacaresse, K. Hynynen and I. Aubert, *J. Controlled Release*, 2022, **351**, 667–680.
93 Y. Touahri, R. Dixit, R. H. Kofoed, K. Mikloska, E. Park, R. Raeisossadati, K. Markham-Coultes, L. A. David, H. Rijal and J. Zhao, *Theranostics*, 2020, **10**, 2982–2999.
94 T. Liu, Q. Wan, C. Zou, M. Chen, G. Wan, X. Liu and H. Chen, *Chem. Eng. J.*, 2021, **417**, 128004.
95 A. Papachristodoulou, R. D. Signorell, B. Werner, D. Brambilla, P. Luciani, M. Cavusoglu, J. Grandjean, M. Silginer, M. Rudin and E. Martin, *J. Controlled Release*, 2019, **295**, 130–139.
96 M. Olsman, V. Sereti, K. Andreassen, S. Snipstad, A. van Wamel, R. Eliasen, S. Berg, A. J. Urquhart, T. L. Andresen and C. de Lange Davies, *J. Controlled Release*, 2020, **325**, 121–134.
97 T.-Y. Shih, A. J. Najibi, A. L. Bartlett, A. W. Li and D. J. Mooney, *Biomaterials*, 2021, **279**, 121240.
98 Y. Li, Y. Qin, Y. Shang, Y. Li, F. Liu, J. Luo, J. Zhu, X. Guo, Z. Wang and Y. Zhao, *Adv. Funct. Mater.*, 2022, **32**, 2112000.
99 F. Zhang, J. Zhuang, B. Esteban, Fernández de ávila, S. Tang, Q. Zhang, R. H. Fang, L. Zhang and J. Wang, *ACS Nano*, 2019, **13**, 11996–12005.
100 D. Wang, C. Gao, W. Wang, M. Sun, B. Guo, H. Xie and Q. He, *ACS Nano*, 2018, **12**, 10212–10220.
101 Y. Chen, M. Du, Z. Yuan, Z. Chen and F. Yan, *Nat. Commun.*, 2022, **13**, 4468.
102 H. Li, X. Li, G. Collado-Lara, K. R. Lattwein, F. Mastik, R. Beurskens, A. F. van der Steen, M. D. Verweij, N. De Jong and K. Kooiman, *Ultrasound Med. Biol.*, 2023, **49**, 388–397.
103 I. Beekers, S. A. Langeveld, B. Meijlink, A. F. van der Steen, N. de Jong, M. D. Verweij and K. Kooiman, *J. Controlled Release*, 2022, **347**, 460–475.
104 Y. Shen, J. Zhang, Y. Xu, S. Sun, K. Chen, S. Chen, X. Yang and X. Chen, *Brain Stimul.*, 2023, **16**, 628–641.
105 J.-Y. Ryu, E.-J. Won, H. A. R. Lee, J. H. Kim, E. Hui, H. P. Kim and T.-J. Yoon, *Biomaterials*, 2020, **232**, 119736.
106 Y.-J. Ho, H.-C. Hsu, B.-H. Wu, Y.-C. Lin, L.-D. Liao and C.-K. Yeh, *J. Controlled Release*, 2023, **356**, 481–492.
107 H. Lea-Banks, Y. Meng, S.-K. Wu, R. Belhadjhamida, C. Hamani and K. Hynynen, *J. Controlled Release*, 2021, **332**, 30–39.
108 G. Wang, Y. Jiang, J. Xu, J. Shen, T. Lin, J. Chen, W. Fei, Y. Qin, Z. Zhou and Y. Shen, *Adv. Mater.*, 2023, **35**, 2207271.
109 K. Fan, L. Zeng, J. Guo, S. Xie, Y. Yu, J. Chen, J. Cao, Q. Xiang, S. Zhang and Y. Luo, *Theranostics*, 2021, **11**, 2670–2690.
110 J. N. Sloand, T. T. Nguyen, S. A. Zinck, E. C. Cook, T. J. Zimudzi, S. A. Showalter, A. B. Glick, J. C. Simon and S. H. Medina, *ACS Nano*, 2020, **14**, 4061–4073.
111 A. Farhadi, G. H. Ho, D. P. Sawyer, R. W. Bourdeau and M. G. Shapiro, *Science*, 2019, **365**, 1469–1475.
112 A. Bar-Zion, A. Nourmahnad, D. R. Mittelstein, S. Shivaei, S. Yoo, M. T. Buss, R. C. Hurt, D. Malounda, M. H. Abedi and A. Lee-Gosselin, *Nat. Nanotechnol.*, 2021, **16**, 1403–1412.
113 D. Wu, D. Baresch, C. Cook, Z. Ma, M. Duan, D. Malounda, D. Maresca, M. P. Abundo, J. Lee and S. Shivaei, *Sci. Adv.*, 2023, **9**, eadd9186.
114 A. Dauba, A. Delalande, H. A. Kamimura, A. Conti, B. Larrat, N. Tsapis and A. Novell, *Pharmaceutics*, 2020, **12**, 1125.
115 M. Du, Z. Chen, Y. Chen and Y. Li, *Curr. Drug Targets*, 2019, **20**, 220–231.
116 H. Zhang, X. Pan, Q. Wu, J. Guo, C. Wang and H. Liu, *Exploration*, 2021, **1**, 20210010.
117 R. Liu, C. Luo, Z. Pang, J. Zhang, S. Ruan, M. Wu, L. Wang, T. Sun, N. Li, L. Han, J. Shi, Y. Huang, W. Guo, S. Peng, W. Zhou and H. Gao, *Chin. Chem. Lett.*, 2023, **34**, 107518.
118 P. Zhao, S. Huo, J. Fan, J. Chen, F. Kiessling, A. J. Boersma, R. Göstl and A. Herrmann, *Angew. Chem., Int. Ed.*, 2021, **60**, 14707–14714.